Preprints (www.preprints.org) | NOT PEER-REVIEWED | Posted: 17 November 2019 doi:10.20944/preprints201911.0211.v1

Polypyrrole-Wrapped Carbon Nanotube Composite Films Coated on Diazonium-Modified Flexible ITO Sheets for the Electroanalysis of Heavy Metal Ions

Momath Lo[1,2,3,*], Mahamadou Seydou[4], Asma Bensghaïer[3], Remy Pires[3], Diariatou Gningue-Sall[1], Jean-Jacques Aaron[2,*], Zineb Mekhalif[5], Joseph Delhalle[5], Mohamed M. Chehimi[3,*]

[1] Université Cheikh Anta Diop, Faculté des Sciences, BP 5005, Dakar-Fann, Sénégal

[2] Université Paris-Est, Laboratoire Géomatériaux et Environnement, 5 Bd. Descartes, 77454 Marne-la-Vallée Cedex 2, France

[3] Univ Paris Est Creteil, CNRS, ICMPE, UMR7182, F-94320 Thiais, France

[4] Univ Paris Diderot, Sorbonne Paris Cité, ITODYS, UMR 7086 CNRS, 15 rue J-A de Baïf, 75205 Paris Cedex 13, France

[5] Laboratory of Chemistry and Electrochemistry of Surfaces (CES), Universityof Namur, rue de Bruxelles, 61, B-5000 Namur, Belgium

Corresponding author (Mohamed M. Chehimi): chehimi@icmpe.cnrs.fr

Abstract

Highly sensitive multicomponent materials designed for the recognition of hazardous compounds request a detailed knowledge of interfacial chemistry. It is a key parameter in the construction of the sensing (macro)molecular architectures. In this work, multi-walled carbon nanotubes (in short, CNTs) were deposited on diazonium-modified flexible ITO electrodes prior to electropolymerization of pyrrole. This three step process, including diazonium electroreduction, deposition of CNTs and electropolymerization, provided adhesively bonded polypyrrole-wrapped CNT composite coatings on aminophenyl-modified flexible ITO sheets. The aminophenyl (AP) groups were attached to ITO by electroreduction of the *in situ* generated aminobenzenediazonium compound in aqueous, acidic medium. For the first time, polypyrrole (PPy) was electrodeposited in the presence of both benzenesulfonic acid (dopant) and ethylene glycol-bis(2-aminoethylether)-tetraacetic acid (EGTA) which acts as a chelator. The flexible electrodes were characterized by XPS, Raman and scanning electron microscopy (SEM) which provided strong supporting evidence for the wrapping of CNTs by the electrodeposited PPy. Indeed, the diameter of the nanotubes increased from 2-9 nm to ~24-35 nm for one voltammetric cycle and further to ~29-45 nm for 5 cycles. The PPy/CNT/NH_2-ITO films generated by this strategy exhibit significantly improved stability and higher conductivity compared to a similar PPy coating without any embedded CNTs as assessed by from electrochemical impedance spectroscopy measurements. The potentiometric response was linear in the 10^{-8}–3×10^{-7} mol.L^{-1} Pb(II) concentration range and the detection limit was 2.9×10^{-9} mol.L^{-1} at S/N=3. The

© 2019 by the author(s). Distributed under a Creative Commons CC BY license.

Preprints (www.preprints.org) | NOT PEER-REVIEWED | Posted: 17 November 2019 doi:10.20944/preprints201911.0211.v1

EGTA was found to drastically improve selectivity for Pb(II) over Cu(II). To account for this improvement, density functional theory (DFT) was employed to calculate the EGTA-metal ion interaction energy which was found to be -374.6 and -116.4 kJ/mol for Pb(II) and Cu(II), respectively, considering solvation effects.
This work demonstrates the power of a subtle combination of diazonium coupling agent, CNTs, chelators and conductive polymers to design high-performance electrochemical sensors for environmental applications.

Keywords: polypyrrole; diazonium; multiwalled carbon nanotubes; chelator; heavy metal ions; electrochemical sensors

1. Introduction

Extensive research on carbon nanotubes (CNTs) in the fields of applied physics, chemistry, and materials science and engineering has progressed at a remarkable pace owing to the CNTs outstanding mechanical properties, good electronic conductivity, 1D structure, nanometer size diameter and high-accessible surface area [1]. In order to design ultra-sensitive sensors, CNTs have been used either as such or after modification by a variety of ways [2,3,4,5].

Conductive polymers (CPs), including polypyrrole (PPy), polyaniline (PANI), and polythiophene (PT), constitute a class of materials which has been widely investigated for their attractive applications in electronic devices [6], super-capacitors [7,8], thermoelectric power generators [9], and gas and ion sensors [10,11,12]. Particularly, PPy and its derivatives play a leading role due to the relative low oxidation potential of the corresponding monomers, high stability and excellent electrical properties in organic and aqueous solvents [13]. Because of these features, PPys are considered as ideal polymeric materials for building various sensors.
In a global effort to combine the best of two worlds, PPy/CNT composites were prepared via chemical [14,15], electrochemical [16], sonochemical [17] and radiation induced routes [18]. Indeed, strong interactions between the highly delocalized - electrons of CNTs and -electrons of the polymer skeleton are favoring the

Preprints (www.preprints.org) | NOT PEER-REVIEWED | Posted: 17 November 2019 doi:10.20944/preprints201911.0211.v1

electron/hole transfer between CNTs and CPs [19,20]. It is worthwhile to note that CNTs impart the polymer film electro-conductivity characteristics which result in fast electrode kinetics and higher electrical conductivity [21]. Taking advantage of the salient and complementary features of CNTs and PPy, various electrochemical sensing systems based on PPy/CNT nanocomposites have been proposed for biomedical and environmental applications [22,23,24,25,26,27].

The main purpose of this work is to rationally modify flexible ITO electrodes with sensitive PPy films, bearing embedded CNTs for the selective recognition of heavy metallic ions. We have previously demonstrated that excellent adhesion of PPy coating on flexible ITO required the use of a coupling agent [28,29]. Otherwise, an immediate failure of the PPy coating occurred upon simple washing of the film with water. Sonication also induced a total delamination. Indeed, excellent adhesion was achieved on aminophenyl-modified ITO electrodes [28], as noted elsewhere for amino-modified materials [30]. For the preparation of composite films of PPy and CNTs, two options are proposed: either polymerization of pyrrole on ITO electrode in a CNT dispersion, or direct polymerization of pyrrole on CNT-coated ITO. The first trials demonstrated that CNTs had a poor adhesion to bare ITO, a behavior similar to that of PPy. To address this limitation and overcome the adhesion problems, flexible ITO electrodes were modified with aminophenyl groups by electroreduction of an aminobenzenediazonium compound. We noted a better adhesion and resistance of CNTs to intensive washing with water and even to ultrasonication. This has motivated us to explore this route in view of building PPy/CNT composite coatings on flexible ITO in three steps: (i) preparation of aminophenyl-modified flexible ITO (NH_2-ITO) [28], (ii) purification and ultrasonic dispersion of CNTs prior to deposition on NH_2-ITO, (iii) electropolymerization of pyrrole in the presence of EGTA on CNT-coated NH_2-ITO.

This strategy presents several advantages: CNTs were deposited on NH_2-ITOby drop casting, which limits the loss of CNTs. Electropolymerization of pyrrole in a CNT

Preprints (www.preprints.org) | NOT PEER-REVIEWED | Posted: 17 November 2019 doi:10.20944/preprints201911.0211.v1

suspension would have generated nanocomposites in suspension that would not adhere to the surface by strong intermolecular interactions. This would lead to leaching the nanocomposite. Instead, coating CNTs on ITO-AP is interesting because the aminophenyl groups serve as coupling agents for CNTs through n electronic interactions. In addition, the protocol adopted so far to attach aminophenyl groups does not exclude the possible transformation of surface bound aminophenyl groups into surface bound benzenediazonium groups since the electrografting is conducted inaHCl/$NaNO_2$ medium. Indeed, carbon materials sp^2 spontaneously react with diazonium compounds [31].

With improved adhesion of CNTs to ITO through a diazonium coupling agent monolayer, we anticipatethat the electropolymerization of pyrrole would yield PPy strongly attached to both the immobilized CNTs and the underlying aryl-modified ITO. Besides this interfacial aspect, in a previous paper, we reported on the doping of PPy with benzenesulfonic acid (BSA) and we obtained remarkable electrochemical and electroanalytical properties of PPy [32]. Herein, we combine BSA with the strong EGTA chelator [33]. The latter is similar to EDTA, but possess an ethylene glycol unit. Since our ongoing research work targets the removal of metal ions, we reasoned expect that EGTA used as chelator would add up two oxygen atoms with 2 electron pairs, which would enhance the complexation of heavy metal ions. Therefore, we combine the versatile surface chemistry of aryl diazonium salts on flexible ITO electrodes, CNTs and electrosynthesized PPy co-doped with BSA and EGTA, which allowed us to construct, in a unique manner, novel NH_2-ITO/CNT/PPy electrodes for the capture of heavy metal ions.

The flexible sensing electrodes and reference materials are characterized using Raman, XPS, SEM and electrochemical impedance spectroscopy. Electroanalytical performances of the sensors are determined by differential pulsed voltammetry (DPV).

Preprints (www.preprints.org) | NOT PEER-REVIEWED | Posted: 17 November 2019 doi:10.20944/preprints201911.0211.v1

2. Experimental

2.1. Material and Reagents.

CNTs of the type Nanocyl 7000, 2-9 nm diameter (carbon purity 99%), were purchased from Sigma Aldrich. Sodium nitrite (Sigma-Aldrich, ≥99.0%), anhydrous acetonitrile (99.8%, noted ACN), chloric acid, ferrocene (Sigma-Aldrich) and potassium chloride were used without further purification. Pyrrole (Aldrich, purity ≥98%), benzene sulfonic acid (BSA) and p-phenylenediamine were refrigerated prior to use. All aqueous solutions were prepared by using Milli-Q ultrapure water (MQ 18.2 cm). The flexible ITO-coated plastic sheets were purchased from Peccel (Japan).

2.2. *In situ*diazonium modification of ITO electrode

We have generated *in situ* para-aminobenzenediazonium cation from 1,4-phenylenediamine precursor in order to derivatize ITO sheets with surface bound aminophenyl groups (NH_2-ITO). The ITO-coated polyethylene naphthalene (ITO-PEN) surface was cleaned by sonication in a solution containing water and ethanol for 2 min. After sonication, the electrode was washed with de-ionized water. The electrografting of diazonium salt generated *in situ* was performed using a three-electrode system, including a working electrode (ITO PEN, area ~ 5x5 mm), and a stainless steel grid, used as counter electrode. All potentials were reported *versus* the Ag/AgCl (saturated KCl) reference electrode. The diazonium salt was produced by mixing 1 mM of diazonium with 0.5 M HCl in glassy beaker during 30 min before adding 10 mL of 1 mM aqueous solution of $NaNO_2$.The resulting solution was stirred for 1h. The electrografting was then carried out either by cyclic voltammetry (CV) at a scan rate of 50 mVs^{-1} or under potentiostatic conditions (-0.8 V/SCE for 45 s). We used a potentiostat Biologic SP 105 controlled by computer with the EC-lab software. The blocking effect of the attached aminophenyl groups as well as the electrochemical activity of the bare and modified ITO electrodes were investigated by

Preprints (www.preprints.org) | NOT PEER-REVIEWED | Posted: 17 November 2019 doi:10.20944/preprints201911.0211.v1

CV using 1 mM $Fe(CN)^{3-/4-}$ redox probe. The CVs were recorded between -0.4 and 0.6 V/SCE at a scan rate of 50 mV / s.

2.3. Purification and deposition of CNTs on diazonium-modified ITO

The process of purification was adapted from [34]. Briefly, 50 mg of crude CNTs was mixed with 20 ml of 6 M NaOH solution in a round-bottomed flask and then heated under constant agitation at 170 C for 1 h. The mixture was cooled, filtered and washed with copious amounts of water until neutral pH and ultimately washed with acetone and dried in air.

In a second step, 25 mg of CNTs were dispersed in 37% HCl solution under reflux for 30 minutes [35]. The mixture was cooled, filtered and washed with water until neutral pH and ultimately washed with acetone and dried in air. This oxidation procedure in concentrated acid is well-known to provide carbon nanotubes with reactive carboxylic acid groups [36].

After activation, 1 mg of purified CNTs was dispersed by ultrasonication in 10mL ACN for 1h. The CNTs/NH_2-ITO electrode surface was obtained by adding 50µL of CNTs in ACN and evaporating the solvent after dropwise addition on NH_2-ITO surface. We observed a strong adherence of the sonicated CNTs on NH_2-ITO surface that allowed us to carry an electropolymerization of pyrrole.

2.4. Preparation of PPy films on ITO surface

Prior to the electropolymerization, CNT-decorated ITO electrodes were sonicated in a solution containing water and ethanol for 2 min. PPy was prepared by electropolymerization on bare ITO (Route 1), NH_2-ITO (Route 2), CNT/NH_2-ITO (Route 3) in the -1 to 1.2 V potential range, in an aqueous solution (~20 ml total volume) containing 0.01 M of BSA, 0.01 M EGTA, 0.03 M NaOH and 0.1 M pyrrole.

2.5. Spectroscopic and electrochemical characterization of PPy-modified electrodes

Preprints (www.preprints.org) | NOT PEER-REVIEWED | Posted: 17 November 2019 doi:10.20944/preprints201911.0211.v1

Measurements were carried out using a Biologic SP105 potentiostat and EC-Lab as a monitoring software. The blocking effect of the electrochemical activity of the modified ITO surface was investigated by CV, using $Fe(CN)^{3-/4-}$ redox couple and recorded between -0.4 and 1 V at a scan rate of 50 mV / s. The electrochemical impedance spectra (EIS) were recorded in the frequency range from 0.1 Hz to 100 kHz.

The film scanning electron microscopy (SEM) data were obtainedusing a LEO Gemini 1530 SEM apparatus (Leo Elektronenmikroskopie, Oberkochen, Germany).

3. Results and Discussion

3.1. Preparation of PPy films on bare ITO, NH_2-ITO and CNT/NH_2-ITO electrodes

Scheme 1 illustrates the strategies for making adhesively bonded PPy films with embedded CNTs on diazonium-modified flexible ITO sheets. The scheme also displays the preparation of reference materials, namely PPy-coated bare ITO and diazonium-modified ITO.

Preprints (www.preprints.org) | NOT PEER-REVIEWED | Posted: 17 November 2019 doi:10.20944/preprints201911.0211.v1

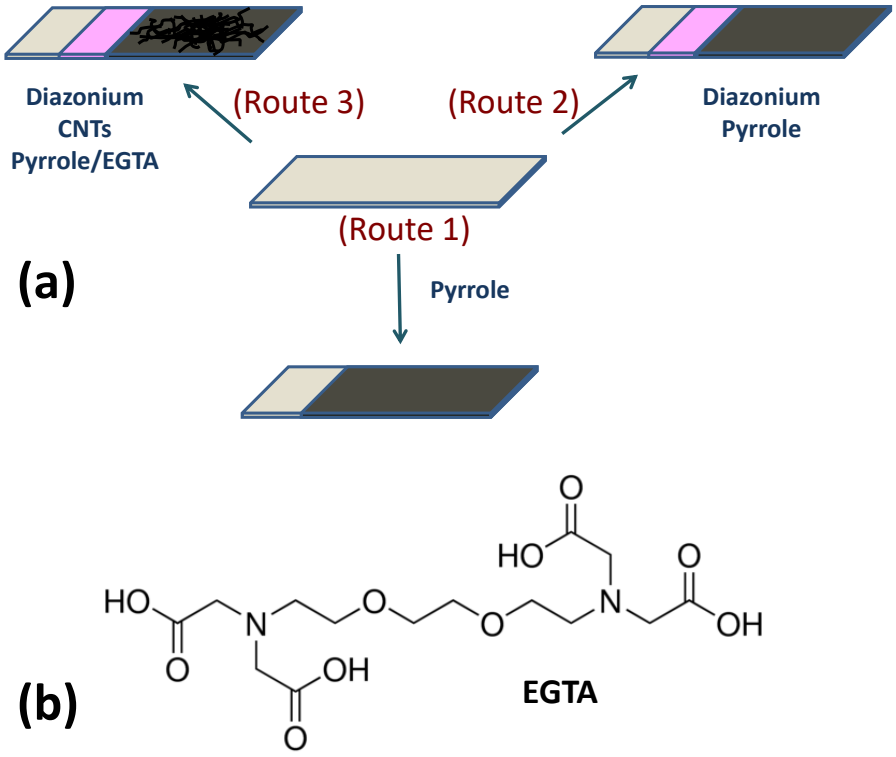

Scheme 1. (a) Procedure for electrodeposition of polypyrrole on bare ITO (Route 1), NH_2-ITO (Route 2), and CNT/NH_2-ITO in the presence of EGTA (Route 3), the structure of which is shown in (b).

Figures 1A-C represent the CVs obtained for the electrosynthesis in similar conditions of the PPy/ITO, PPy/NH_2-ITO, and PPy/CNTs/NH_2-ITO films, respectively. The CVs have been performed for ten sequential cycles, at a scan rate of 0.1 V s^{-1}, in the potential range (-1.0 to 1.2 V/SCE) in aqueous medium ~20 ml total volume containing 0.01 M of BSA, 0.01 M of EGTA, and 0.03M of NaOH. The characteristic CV of pyrrole electropolymerization on bare ITO electrodes (Figure 1A) presents anodic and cathodic peaks at 0.34 and -0.25V/SCE, respectively. The PPy film, prepared in these conditions on bare ITO, is not adherent and can be easily removed which contrasts with the remarkable adhesion of PPy films prepared on NH_2-ITO (Figure 1B). The peak at about +0.35 V/SCE corresponds to the oxidation of pyrrole on ITO-NH_2 and increases with the number of cycles. The increase in the intensity of the oxidation and reduction peaks (at 0.4 and − 0.12 V/SCE, respectively) with the number of cycles is consistent with the growth of an electroactive PPy

Preprints (www.preprints.org) | NOT PEER-REVIEWED | Posted: 17 November 2019 doi:10.20944/preprints201911.0211.v1

coating [37]. Furthermore, the peak currents have higher intensities for the same system for PPy on a CNT/NH_2-ITO surface (Figure 1C). The highly adherent PPy films on CNT/NH_2-ITO surfaces exhibit anodic and cathodic peaks at 0.25 and -0.85 V/SCE which increases with the number of cycles. These differences in electroactivity *versus* the substrate nature clearly indicate that the PPy coating deposited on CNT/NH_2-ITO is the most conducting one. These results are in line with the reported results of Pilan *et al*. [38] in their study of polyaniline/carbon nanotube composite film electrosynthesis through diazonium salts electroreduction.

Preprints (www.preprints.org) | NOT PEER-REVIEWED | Posted: 17 November 2019 doi:10.20944/preprints201911.0211.v1

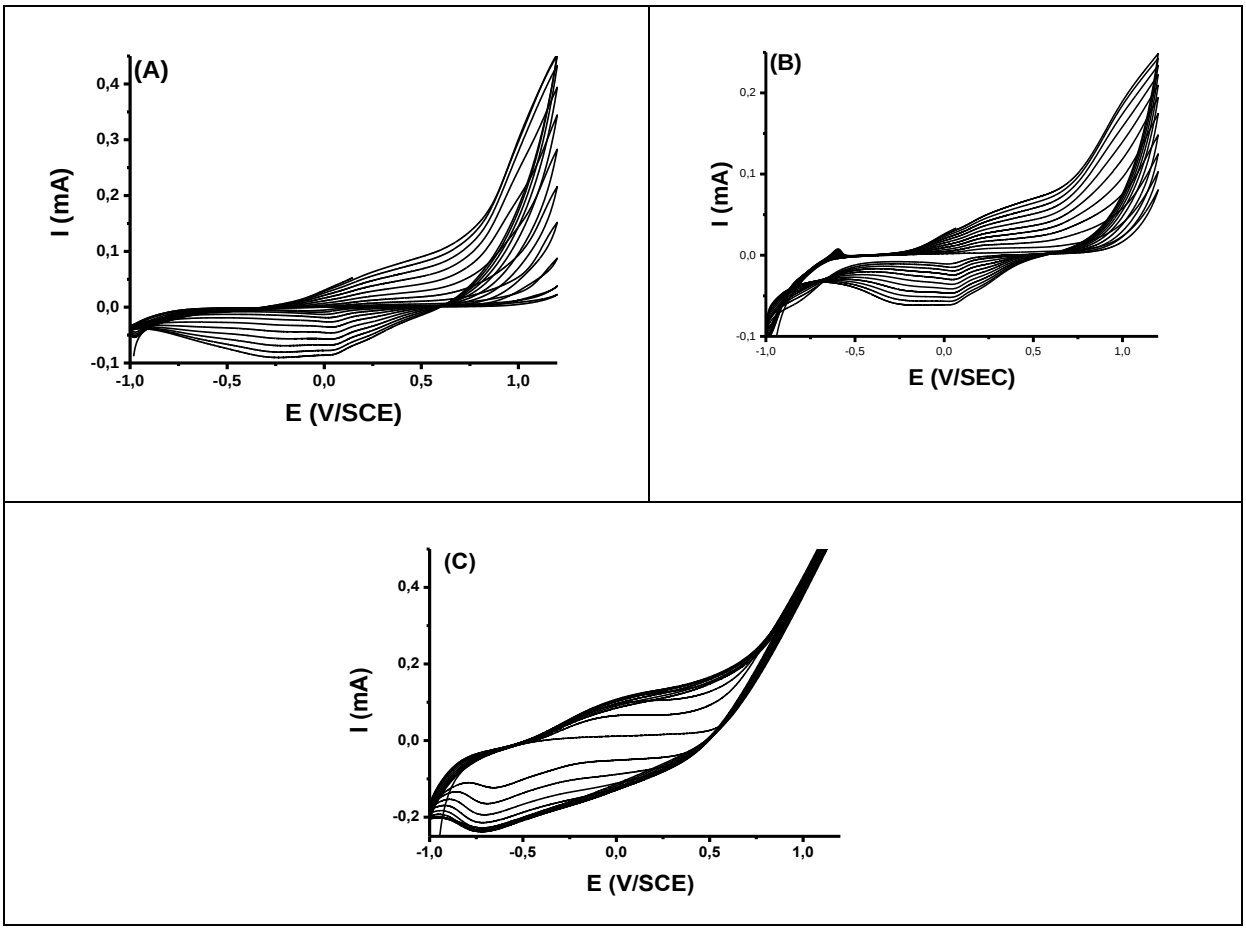

Figure 1. Electropolymerization of PPy on (A) bare ITO, (B) NH_2-ITO, and (C) CNTs/NH_2-ITO.

3.2. Structural characterization of modified flexible ITO sheets

3.2.1. Electrochemical properties

$Fe(CN)^{3-/4-}$ has been used as redox probe to characterizePPy-ITO, PPy/NH_2-ITO, PPy/CNT/NH_2-ITO by CV and EIS (Figure 2).

From CV (Figure 2A), one can extract the potential difference between the anodic and the cathodic peaks, which is high for PPy films deposited on bare ITO: $\Delta E = | E_{red} - E_{ox} | = 430$ mV. This difference can be linked to the absence of any adhesion between the PPy layer and the bare ITO surface [28]. In the case of PPy/NH_2-ITO, the presence of -NH_2 on ITO contributes to increase the electronic transfers leading to a lower ΔE (181 mV). For PPy/CNT/NH_2-ITO, $\Delta E = 321$ mV. The

Preprints (www.preprints.org) | NOT PEER-REVIEWED | Posted: 17 November 2019 doi:10.20944/preprints201911.0211.v1

CV results are consistent with those obtained by EIS (Figure 2B). Indeed, EIS shows a low resistivity in the case of PPy/CNT/NH_2-ITO, a significant blocking effect (increase of Rct) in the case of PPy-ITO, and a decrease of the resistivity character in the case PPy/NH_2-ITO. The following Rct values were obtained: 2250, 690 and 445 Ohms for PPy/ITO, PPy/NH_2-ITO and PPy/CNT/NH_2-ITO, respectively. In conclusion, the presence of a PPy layer on CNT/NH_2-ITO surface leads to an increase of the electronic transfers due to the presence of the p-CNTs in the layer.

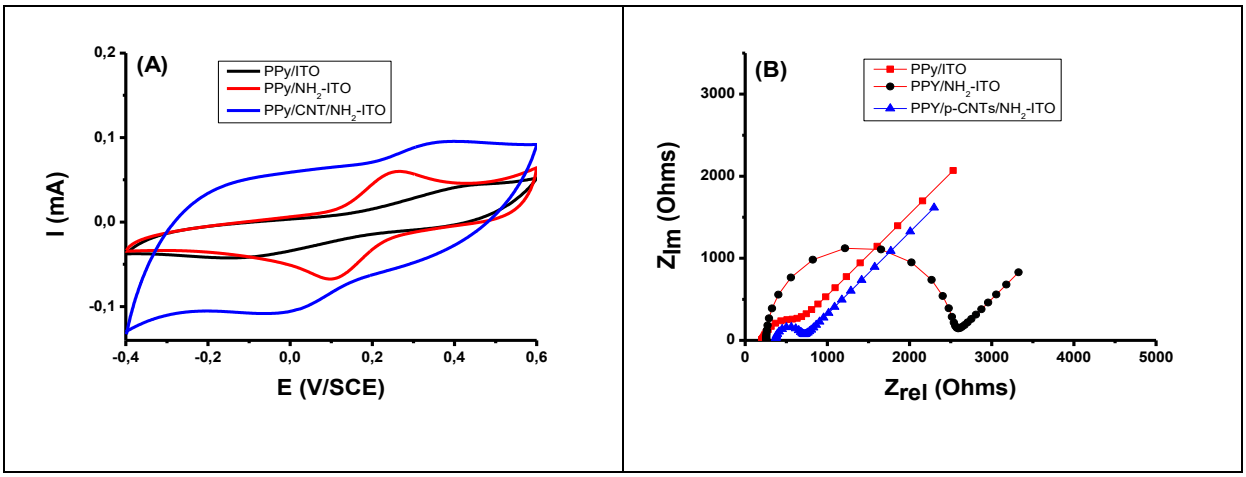

Figure 2. (A) Cyclic voltammograms, and (B) Nyquist plots of electrochemical impedance spectra obtained for PPy-ITO, PPy/NH_2-ITO, PPy/CNTs/NH_2-ITO. For CV: scan rate of 50 mV s^{-1}; for EIS: within the frequency range of 100 mHz-10 kHz.

3.2.2. Raman study of modified flexible ITO sheets

Figure 3 shows the Raman spectra of NH_2-ITO, CNT/NH_2-ITO and PPy/CNT/NH_2-ITO. The NH_2-ITO sample exhibits Raman bands due to the aryl groups, centered at 1387 and 1632 cm^{-1}, assigned respectively to the C-H and C=C bonds in benzene ring. The band located at 1104 cm^{-1} is assigned to C-H in-plane vibrations and the band at 1282 cm^{-1} is due to the C-N stretching vibration [39].

The Raman spectra of CNTs deposited on the aryl diazonium layer show the most prominent features, i.e. the D band, associated with the defects in the hexagonal graphitic layers, and the G band, related to the vibrations of sp^2-bonded carbon

Preprints (www.preprints.org) | NOT PEER-REVIEWED | Posted: 17 November 2019 doi:10.20944/preprints201911.0211.v1

atoms in a two-dimensional hexagonal lattice. The D and G bands are centered at 1337 and 1587 cm^{-1}, respectively, with the ID/IG peak intensity ratio of 1.21 for CNT/NH_2-ITO. These results suggest that the surface treatment with the aryl diazonium salt does not affect the structure of the CNTs [17] and confirm that the aryl groups are interacting with CNTs *via* van der Waals and H bondings.

The PPy coated on CNT/NH_2-ITO surface exhibits a band at 1332 cm^{-1} attributed to the ring-stretching mode of PPy, whereas the peak at 1566 cm^{-1} is assigned to the backbone stretching mode of C=C bonds with the ID/IG peak intensity ratio 1.05 [40]. The Raman spectra of PPy are similar to those obtained by Song *et al.* [40] and reveal that CNTs serve as the core in the formation of CNT/PPy composites.

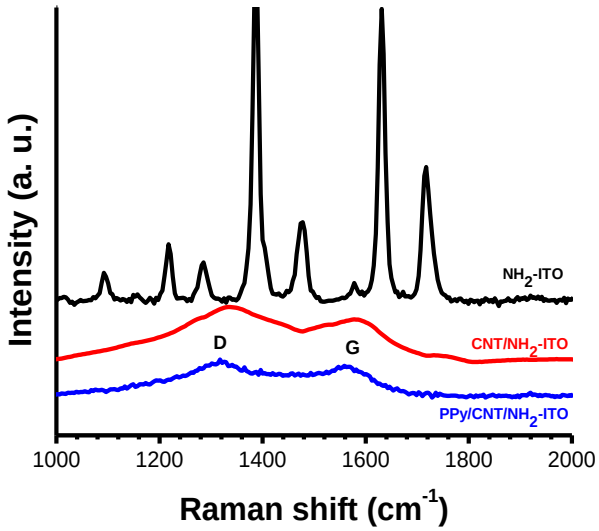

Figure 3. Raman spectra of NH_2-ITO, CNT/NH_2-ITO, PPy/CNT/NH_2-ITO

3.2.3. Morphology characterization of modified flexible ITO sheets

Figures 4a-d show SEM images of CNT/NH_2-ITO, PPy/CNT/NH_2-ITO, formed by CV for 1, 5 and 10 cycles. The SEM images of areas filled with CNTs (Fig. 4a) further demonstrates that the tubes are homogeneous and can be distinguished individually with a nanometer scale width. In Figure 4b, the SEM images of PPy on CNT/NH_2-

Preprints (www.preprints.org) | NOT PEER-REVIEWED | Posted: 17 November 2019 doi:10.20944/preprints201911.0211.v1

ITO formed after one CV does not change the arrangement of CNTs, but preferentially wraps around them, one by one.When the number of cycles increases to 5 (Figure 4c) and 10 (Figure 4d), the CNTs thicken gradually and homogeneously due to the wrapping by PPy. For 10 voltammetric cycles, the PPy/CNT/NH_2-ITO film exhibit compact filaments with persisting three-dimensional porous microstructure composed of fibrils [41]. Interestingly, there is no side deposition of PPyindicating that the electrosynthesis of the polymer is confined to the sidewalls of the nanotubes, therefore suggesting strong interactions between PPy and the underlying CNTs.

CNTs diameters distributions for 0, 1, 5and 10 CVs of PPy electrodeposition are shown in the insets of Figures 4a-d. The CNT average diameter is 17.8 nm (Figure 4a). After 1 cycle, the CNT diameter increases to 20-46.5 nm range (Figure 4b) with a distribution around 26.1 nm. After 5 cycles (Figure 4c) the CNT diameter increases to 25.1-63.0 nm with a median value of 34.6 nm, and finally 126-233 nm with a median value of 176 nm after 10 cycles of electropolymerization. These results confirm that the deposition of PPy is mostly confined to the CNT sidewalls.

The interface between CNTs and NH_2-ITO has been study by SEM (Figure 5). The attachment of CNTs on the NH_2-ITO surface can be noted, thus proving the interaction of the carbon nanotubes and diazonium-modified ITO [42,43]. The SEM morphology for the interface betwenPPy and CNT/NH_2-ITO (Figure 5b) shows that the PPy wraps around the CNTs [38] therefore confirming the structures displayed in Figure 4.

Preprints (www.preprints.org) | NOT PEER-REVIEWED | Posted: 17 November 2019 doi:10.20944/preprints201911.0211.v1

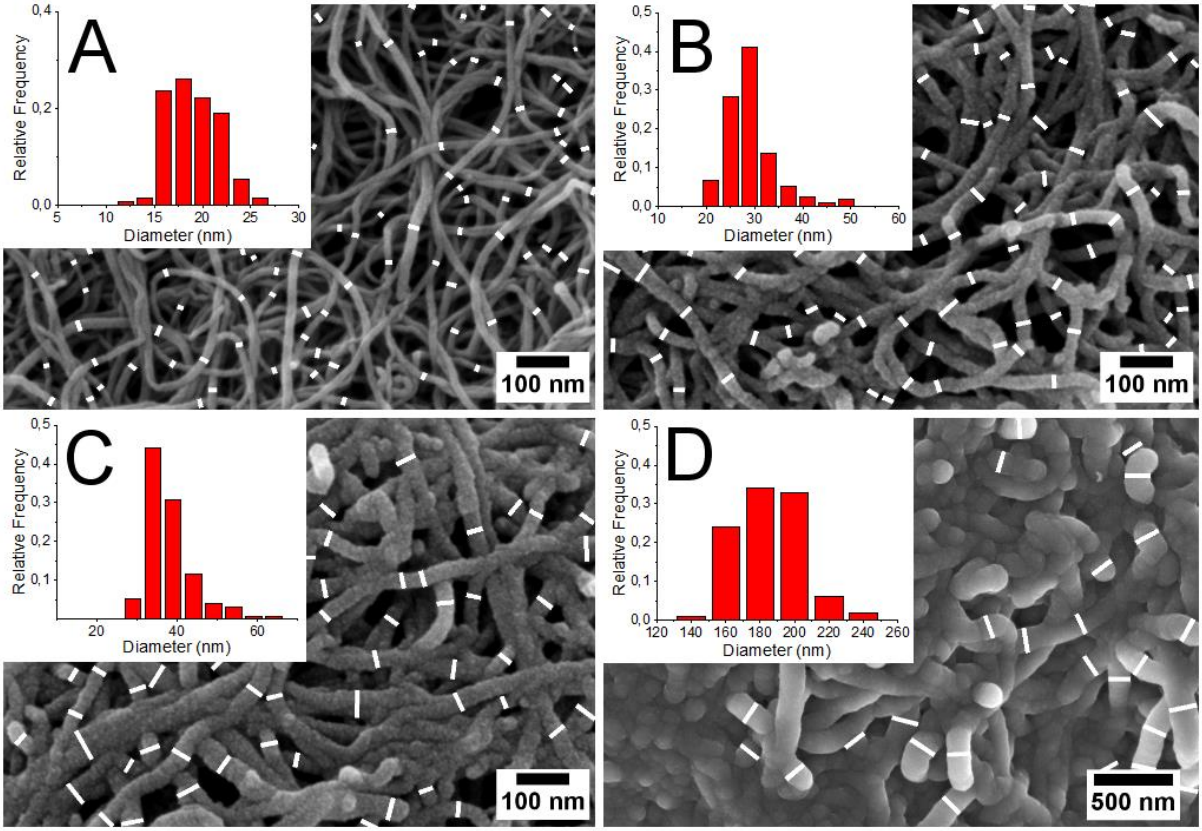

Figure 4. CNT size distribution. Histogram of the relative frequency versus the CNT diameters determined. (a) CNT/NH_2-ITO, (b) PPy/CNT/NH_2-ITO formed by CV for 1 cycle, c) PPy/CNT/NH_2-ITO formed by CV for 5 cycles, d) PPy/CNT/NH_2-ITO formed by CV for 10 cycles.

Preprints (www.preprints.org) | NOT PEER-REVIEWED | Posted: 17 November 2019 doi:10.20944/preprints201911.0211.v1

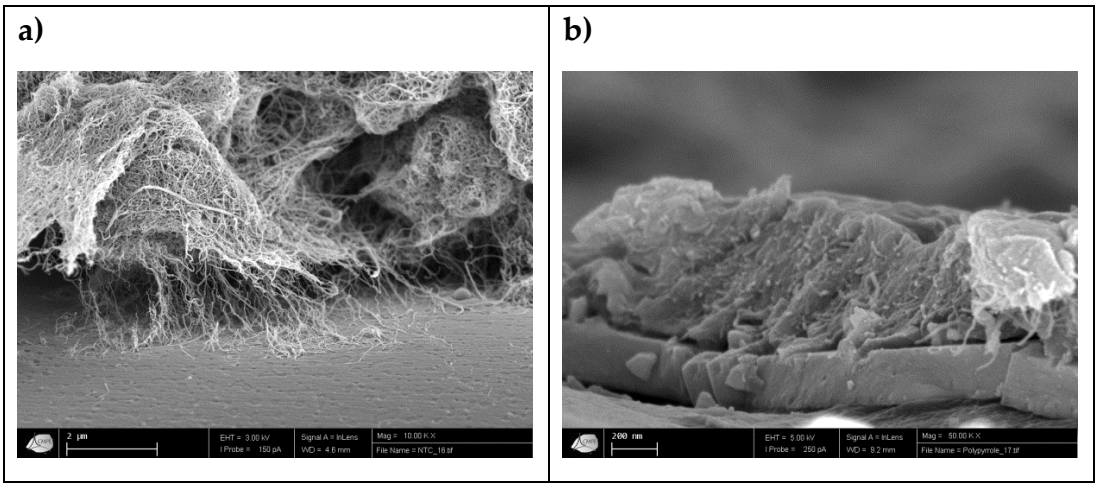

Figure 5. SEM images of (a) interface between MWCNTs and NH_2-ITO, (b) Interface between PPy-wrapped CNTs and NH_2-ITO.

3.3. Electroanalytical application of PPy/CNT/NH_2-ITO electrodes

The electrochemical response was assessed in the same electrolytic solution containing 10^{-7} mol.L^{-1} of Pb^{2+}, using two different modified electrodes: PPy/CNT/NH_2-ITO and PPy/NH_2-ITO (Figure 6A). It is worth noticing that the peak current obtained for PPy/CNT/NH_2-ITO present a higher value than that obtained for PPy/NH_2-ITO, due to the conductivity increaseinduced by the CNTs to the PPy matrix. As reported elsewhere, CNTs might enhance the diffusion rate of heavy metal ions during the sensing measurements [44].

The effect of pre-concentration time on the DPV current is demonstrated in Figure 6B. The stripping peak current for both metals increased with the pre-concentration time increasesup to 10 min.For periods longer than 10 min, the peak current was almost constant, which might be due to the electrode saturation by Pb^{2+}. Therefore, the value of 10 min was chosen as the pre-concentration time.

PPy/CNT/NH_2-ITO samples served to detect lead ions in an aqueous medium by differential pulse voltammetry (DPV) (Figure 6C). This figure displays DPV signals for Pb^{2+} concentrations in the 10^{-8} to 3×10^{-7} mol.L^{-1} range (I (µA) = 1.5 C + 1.64, R= 0.996). LOD is deduced from the DPV peak intensity-*vs*-concentration correlation (inset of Fig. 6C); LOD=2.9×10^{-9}mol.L^{-1} and the limit of quantification LOQ = 8.7×10^{-9}mol.L^{-1}at S/N=3.

Preprints (www.preprints.org) | NOT PEER-REVIEWED | Posted: 17 November 2019 doi:10.20944/preprints201911.0211.v1

Preprints (www.preprints.org) | NOT PEER-REVIEWED | Posted: 17 November 2019 doi:10.20944/preprints201911.0211.v1

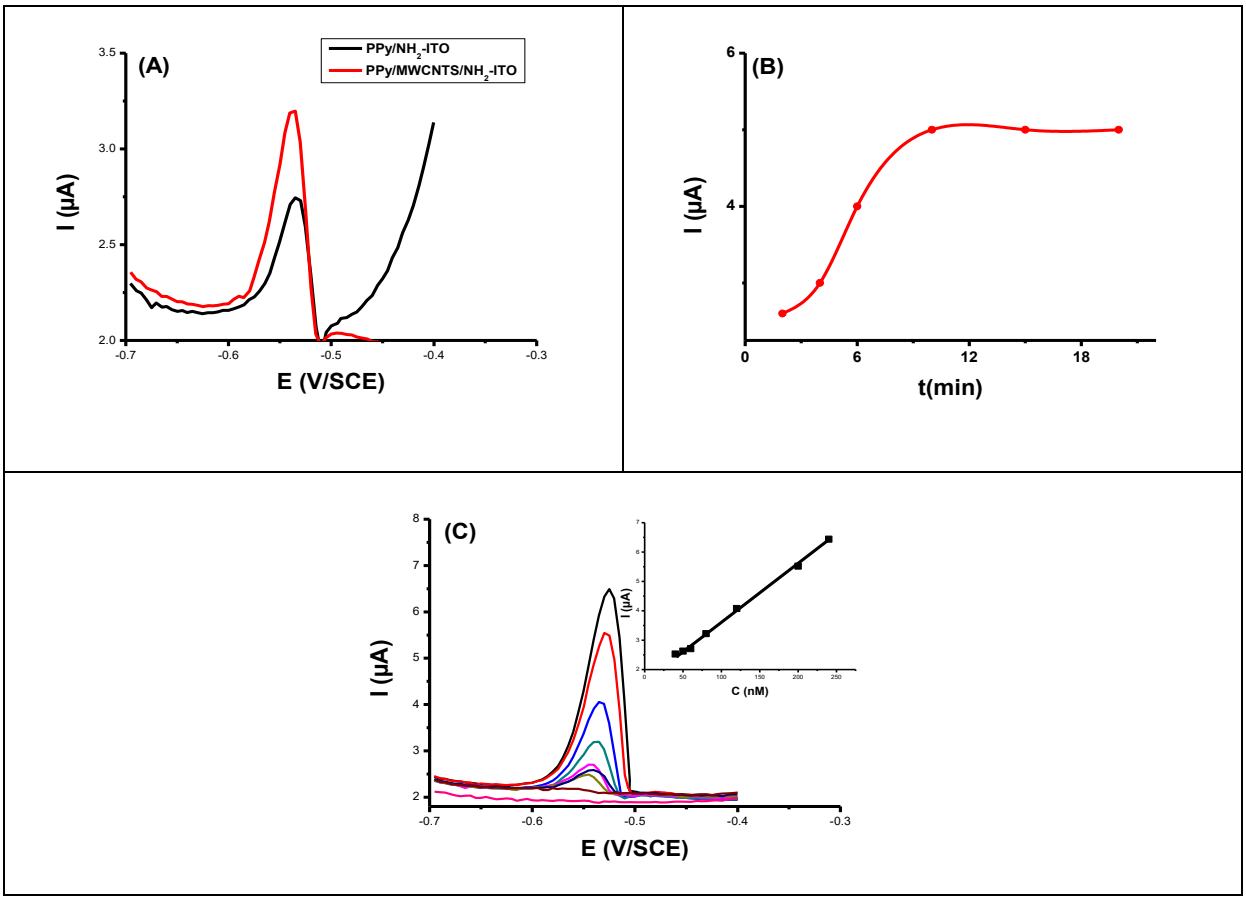

Figur 6. (A)DPV of Pb(II) at pH 5 containing Pb(II) 10^{-7}mol.L^{-1}for PPy/CNT/NH$_2$-ITO and PPy/NH$_2$-ITO, (B) Time effect of pre-concentation metal ion on PPy/CNT/NH2-ITO, (C) various Pb(II) concentrations in the 10^{-8}-2.5x10^{-7} mol.L^{-1} range. Calibration curve (Inset of Fig. 6C).

At this stage, the question concerning the use of EGTA remains open: how useful is this chelator? Previously, we have shown that without any CNTs and EGTA, the LOD is ~ 1×10^{-9}mol.L^{-1}, which is slightly better. However, with CNTs, a better conductivity of the sensing top layer is obtained. Concerning EGTA, we have investigated the selectivity of the film towards Pb^{2+} and Cu^{2+}. According to our previously published procedure [32], we have determined, for a total initial concentration of metal ions of 2.5×10^{-6} mol.L^{-1}, the relative intensity of Pb^{2+} stripping peak, in the presence and in the absence of interfering Cu^{2+} ions, at various initial Cu^{2+}/Pb^{2+} molar ratio. The electrochemical response is displayed in Figure 7. As it can be seen, it clearly exhibits two well resolved stripping peaks, respectively assigned to Pb^{2+} and to Cu^{2+}. Inset of

Preprints (www.preprints.org) | NOT PEER-REVIEWED | Posted: 17 November 2019 doi:10.20944/preprints201911.0211.v1

Figure 7 plots the Pb peak intensity ratio I_s/I_0 (in %), where I_s and I_0 stand for the stripping peak of Pb^{2+} in the presence and absence of Cu^{2+} interfering cations, respectively. Obviously, with EGTA, despite the presence of Cu^{2+}, the stripping response of Pb^{2+} does not decrease significantly, hence the interest of performing the PPy electrosynthesis in the presence of EGTA, as co-dopant and chelator.

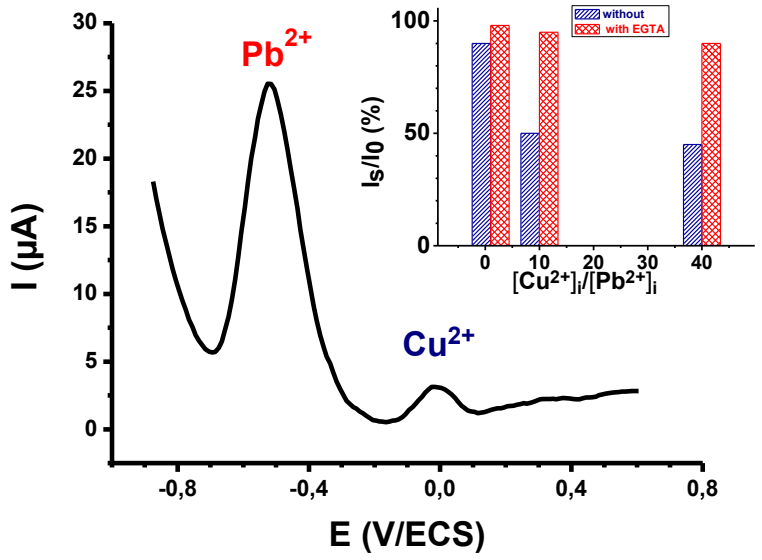

Figure 7. DPV simultaneous determination of concentration 2.510^{-6} M of a Pb^{2+} and Cu^{2+} mixture with initial Cu^{2+}/Pb^{2+} molar ratio = 1. Inset shows that for $[Cu^{2+}]_i/[Pb^{2+}]_i$ = 1, 10, 40, I_s/I_0= 90, 50 and 45, respectively, without EGTA; whilst I_s/I_0=98, 95 and 90, respectively, in the presence of EGTA.

3.4. Density functional theory calculations

Quantum chemical calculations are realized by using density functional theory (DFT) at B3LYP/6-31+G* level by using 6-311+G(d) basis set for H, C, N, O atoms and LANL2DZ basis set for Cu an Pb atoms as implemented in Gaussian16 [45,46].

The solvent effect was added by using the United Atom molecular cavity model UAKS (united atom Kohn–Sham model) [47]. The formation energy of the complexes in gas phase and in solvent is computed from Hess thermodynamic cycle (Scheme 2). The gas phase ionization energy is extracted from reference [48].

Preprints (www.preprints.org) | NOT PEER-REVIEWED | Posted: 17 November 2019 doi:10.20944/preprints201911.0211.v1

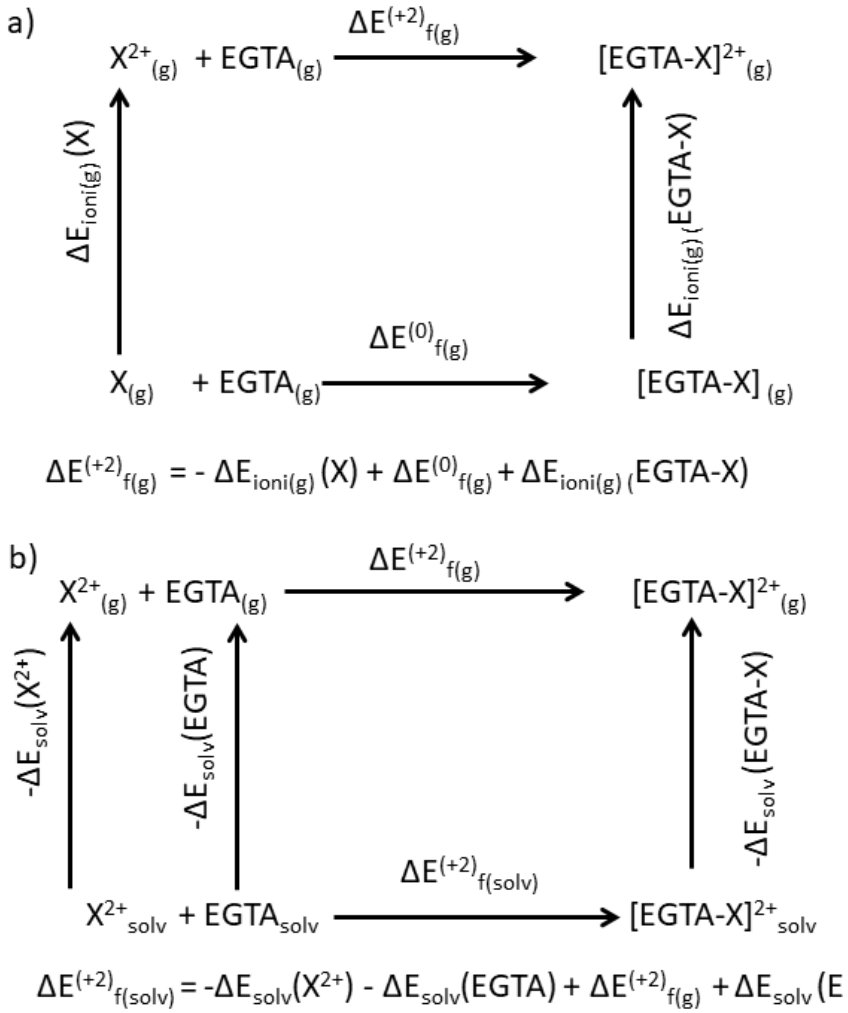

Scheme 2. Termodynamic cycles used to calculate the complexation energy in gas (a) and in solvent (b).

An exhaustive conformational search is explored for EGTA molecule in order to determine the most stable structure. The most stable configuration is stabilized by hydrogen bonds between carboxylic acid groups as it can be seen on Figure 8. This conformer is used to complex with Cu^{2+} and Pb^{2+} ions. The formed complexes are fully optimized and the formation energies are computed in both gas and liquid phases. In gas phase, the calculated complexation energy was found to be-802.4 kJ/mol and –741.9 kJ/mol for Pb^{2+} and $Cu^{2+,}$ respectively. When adding solvent effect, the values decrease to -374.6 and -116.4 kJ/mol for Pb^{2+} and Cu^{2+}, respectively. The difference is linked to the more favorable complexation in the gas phase of Pb^{2+} and

Preprints (www.preprints.org) | NOT PEER-REVIEWED | Posted: 17 November 2019 doi:10.20944/preprints201911.0211.v1

the important solvation of Cu^{2+} (Table 1). Based on these thermodynamics results, one can conclude that the formation of Pb^{2+} complex is more favorable compared to Cu^{2+}. The optimized geometries of complexes are presented in Figure 8 and show different type of coordination for the two ions. The Pb^{2+} ion is hexa-coordinated with forth O-Pb bonds varying between 2.452 and 2.662 Å close the sum of Pb and O atomic radius (2.44 Å). It is bonded to nitrogen atoms at distances 2.854 and 2.903 larger than the sum of atomic radii of isolated elements. The Cu^{2+} ion is penta-coordinated with four oxygen and one nitrogen atoms. The bond length of Cu-O varies between 2. 04 and 2.23 Å are closed to the sum of atomic radius of Cu and O (2.01 Å). The Cu-N bond length is 2.13 Å, larger than the sum of atomic radii of Cu and N (2.03 Å).

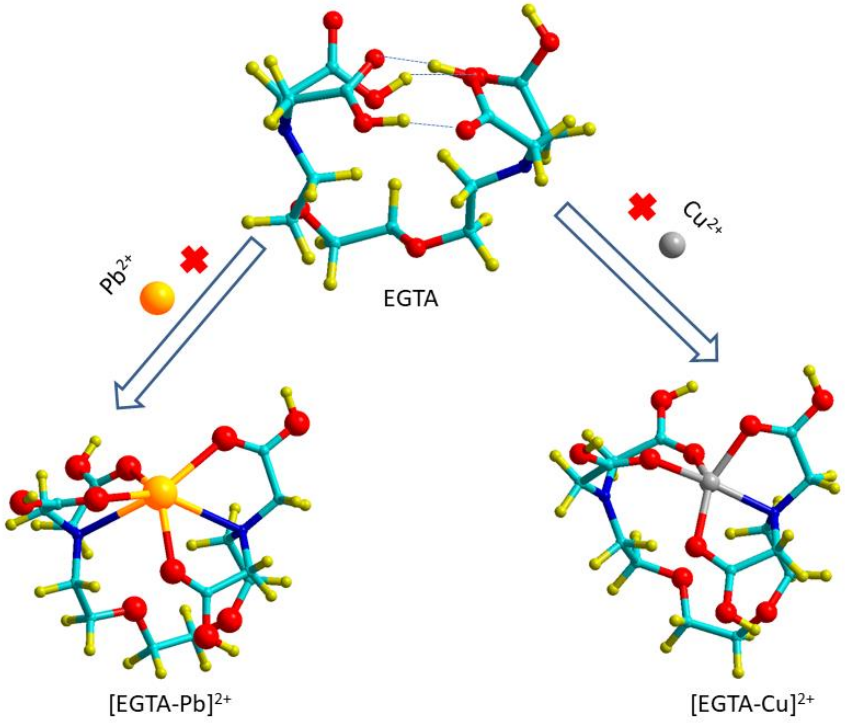

Figure 8. Structures of stable conformers of EGTA and,$[EGTA\text{-}Pb]^{2+}$ and $[EGTA\text{-}Cu]^{2+}$ complexes.

Table 1. Formation energies in gas phase ($\Delta E^{(+2)}_{f(g)}$), in solvent ($\Delta E^{(+2)}_{f(solv)}$), solvation energies and X-O and X-N minimum and maximum distances for the most stable complexes.

Preprints (www.preprints.org) | NOT PEER-REVIEWED | Posted: 17 November 2019 doi:10.20944/preprints201911.0211.v1

System	$\Delta E^{(+2)}_{f(g)}$ (kJ/mol)	ΔE_{solv}(kJ/mol)	$\Delta E^{(+2)}_{f(solv)}$ (kJ/mol)	dX-O (Å)	dX-N (Å)
EGTA	-	-127.8	-	-	-
Cu^{2+}	-	-1288.8	-	-	-
Pb^{2+}	-	-1038.8	-	-	-
$[EGTA\text{-}Cu]^{2+}$	-741.9	-790.9	-116.4	2.047 (2.238)	2.135 (3.574)
$[EGTA\text{-}Pb]^{2+}$	-802.4	-738.8	-374.6	2.452 (2.662)	2.854(2.903)

Conclusion

PPy/CNT/NH_2-ITO composites have been prepared by electropolymerization on diazonium-modified flexible ITO electrodes coated with CNTs, in the presence of the EGTA chelator. The conductive polymer was also prepared by electropolymerizationon NH_2-ITO and on bare ITO without any CNTs. CNTs were easily removed from ITO, but resisted solvent washing on NH_2-ITO flexible electrodes. Electrodeposition of PPy was found to be confined to the CNTs sidewalls as evidenced by SEM and the growth of the CNT diameter with the number of voltammetric cycles used to generate polypyrrole. The electropolymerizationof PPy on CNTs surface exhibits more expanded molecular conformation and more ordered chain packing, due to the strong π–π and n-π conjugation interactions between PPy and CNTs and the efficient template effect of CNTs during the electropolymerization. The increase of the electrochemical conductivity has been observed in the PPy deposited on CNT/NH_2-ITO.

The PPy/CNT/NH_2-ITO composite electrodes were used for the electroanalysis of Pb^{2+} in aqueous media. The LOD was found to be 2.9×10^{-9} $mol.L^{-1}$ at S/N=3. Interestingly, EGTA was found to drastically improve the selectivity of the sensor towards Pb^{2+}, as the response of the EGTA-containing sensor did not change even in the presence of relatively large concentration of competitive Cu^{2+} metal ions. Such improved selectivity imparted by EGTA is due to the higher EGTA-Pb^{2+} interaction energy (-374.6 kJ/mol) compared to that of EGTA-Cu^{2+} (-116.4 kJ/mol) as judged from DFT calculations that consider solvation effects.

Preprints (www.preprints.org) | NOT PEER-REVIEWED | Posted: 17 November 2019 doi:10.20944/preprints201911.0211.v1

This work demonstrates conclusively the importance of diazonium salts to improve CNTs adhesion to ITO electrode surfaces serving as template for the *in situ* polypyrrole electrodeposition. The embedded CNTs impart remarkable properties to the polypyrrole sensing layers the selectivity of which is drastically improved using the EGTA chelator.

Acknowledgements
ML gratefully thanks the Cooperation and Cultural Action Service of the French Embassy in Senegal for a PhD grant. AB and MMC wish to thank NATO for financial support through the CATALTEX project No SfP 984842. All authors acknowledge Wallonie-Bruxelles International (Belgium) for the provision of a grant to ML within the framework of "Programme de Bourses d'Excellence".

Author Contributions:
Conceptualization of the research work by M.L., M.M.C. and D.G.-S.
Methodology by M.L., A.B. MS, and M.M.C.;
Validation by M.M.C., R.P., M.S., D.G.-S., J.-J.A., ZM, JD;
Formal Analysis by M.L., R.P., M.S., M.M.C., Z.M.;
Writingof Original Draft was done by M.L., M.S. and M.M.C.;
Writing: Review and Editing, M.L., M.M.C., J.-J.A., Z.M., J.D.;
Supervision, M.M.C., D.G.-S., Z.M.;
Funding Acquisition, J.-J.A., D.G.-S., Z.M.

Preprints (www.preprints.org) | NOT PEER-REVIEWED | Posted: 17 November 2019 doi:10.20944/preprints201911.0211.v1

REFERENCES

[1] Iijima, S.; Ichihashi, T.; Single-shell carbon nanotubes of 1-nm diameter. *Nature*.**1993**, 364, 603-737.

[2] Al-Harbi, E. A. ; Abdelrahman, M. H. ; El-Kosasy, A. M. ; Ecofriendly Long Life Nanocomposite Sensors for Determination of Carbachol in Presence of Choline: Application in Ophthalmic Solutions and Biological Fluids. *Sensors* **2019**, *19*, 2357.

[3] George J.; Abdelghani, A.; Bahoumina, P.;Tantot, O.; Baillargeat, D.; Frigui, K.; Bila, S.; Hallil, H.; Dejous, C.; CNT-Based Inkjet-Printed RF Gas Sensor: Modification of Substrate Properties during the Fabrication Process. *Sensors* **2019**, *19*, 1768.

[4] Liu, Z.; Yang, T.; Dong, Y.; Wang, X.; A Room Temperature VOCs Gas Sensor Based on a Layer by Layer Multi-Walled Carbon Nanotubes/Poly-ethylene Glycol Composite. *Sensors* **2018**, 18, 3113.

[5]. Wang, J.; Du, S.; Onodera, T.; Yatabe, R.; Tanaka, M.; Okochi, M.; Toko, K.; An SPR Sensor Chip Based on Peptide-Modified Single-Walled Carbon Nanotubes with Enhanced Sensitivity and Selectivity in the Detection of 2,4,6-Trinitrotoluene Explosives. *Sensors* **2018**, 18, 4461.

[6] Sun, X.; Zhang, H.; Zhou, L.; Huang, X.; Yu, C. Polypyrrole-Coated Zinc Ferrite Hollow Spheres with Improved Cycling Stability for Lithium-Ion Batteries. *Small*. **2016**, 12, 3732–3737.

[7] Chen, S.; Zhitomirsky, I. Strategies to Optimize the Capacitive Behavior of Polypyrrole Electrodes.*Mater. Manuf. Processes.***2016**, 31, 2017–2022.

[8] Chen, S.; Zhitomirsky, I. Influence of Additives on Performance of Polypyrrole-Carbon Nanotube Supercapacitors. *Mater. Manuf. Processes*. **2016**, 31, 1246– 1252.

[9] Bharti, M.; Singh, A.; Samanta, S.; Aswal, D.K.; Conductive polymers: Creating their niche in thermoelectric domain, *Prog. Mater. Sci.***2018**, 93, 270-310.

[10]Kotresh, S.; Ravikiran, Y.; VijayaKumari, S.; Chandrasekhar, T.; Ramana, C.V.; Thomas, S. Solution-based Spin Cast Processed Polypyrrole/Niobium Pentoxide Nanocomposite as Room Temperature Liquefied Petroleum Gas Sensor. *Mater. Manuf. Processes*. **2016**, 31, 1976–1982.

[11]Muliwa, A.M.; Leswifi, T.Y.; Onyango, M.S.; Maity, A. Magnetic Adsorption Separation (MAS) Process: An Alternative Method of Extracting Cr (VI) from Aqueous Solution using Polypyrrole Coated Fe3O4 Nanocomposites. *Sep. Purif. Technol*. **2016**, 158, 250–258.

[12] Bhaumik, M.; Agarwal, S.; Gupta, V.K.; Maity, A. Enhanced Removal of Cr (VI) from Aqueous Solutions using Polypyrrole Wrapped Oxidized MWCNTs Nanocomposites Adsorbent. *J. Colloid Interface Sci*. **2016**, 470, 257–267.

[13]Sadki, S.; Schottland, P.; Brodie N.; Sabouraud, G. The mechanisms of pyrrole electropolymerization, *Chem. Soc. Rev*. **2000**, 29, 283–293

[14]Wu, T.M.; Lin, S.-H.; Characterization and electrical properties of polypyrrole/multiwalled carbon nanotube composites synthesized by in situ chemical oxidative polymerization. *J. Polym. Sci Part B.***2006,** 44,1413–1418

[15] Park, S.J.; Kwon, O.S., Jang, J. A high-performance hydrogen gas sensor using ultrathin polypyrrole-coated CNT nanohybrids. *Chem. Commun.*, 2013, **49**, 4673-4675.

Preprints (www.preprints.org) | NOT PEER-REVIEWED | Posted: 17 November 2019 doi:10.20944/preprints201911.0211.v1

[16] Lu, Y.; Li, T.; Zhao, X.; Li, M.; Cao, Y.; Yang, H.; Duan, Y.Y. Electrodeposited polypyrrole/carbon nanotubes composite films electrodes for neural interfaces. *Biomaterials.***2010**, 31, 5169-5181.

[17] Hamouma, O.; Oukil, D.; Omastovà, M.; Chehimi, M.M. Flexible paper@carbonnanotube@polypyrrole composites: The combined pivotal roles of diazonium chemistry and sonochemical polymerization. *Colloids Surf. A.***2018**, 538, 350-360

[18]Karim, M.R.; Lee C.J.; Chowdhury, A.M.S.; Nahar, N.; Lee, M. S. Radiolytic synthesis of conducting polypyrrole/carbon nanotube composites. *Mater. Lett.***2007**, 61, 1688–1692.

[19] Rahman, G.M.M.; Guldi, D.M.; Cagnoli, R.; Mucci, A.; Schenetti, L.; Vaccari, L.; Prato, M. Combining single wall carbon nanotubes and photoactive polymers for photoconversion. *J. Am. Chem. Soc.***2005,** 127, 10051- 10057.

[20] Cochet, M.; Maser, W.K.; Benito, A.M.; Callejas, M. A.M.; Martinez, T.; Benoit, J.M.; Schreiber, J.; Chauvet, O. Synthesis of a new polyaniline/nanotube composite:“in-situ” polymerisation and charge transfer through site-selective interaction. *Chem. Commun*. **2001**, 0, 1450-1451.

[21]Bayrakçeken, H.; Naktiyok, J.; Özer, A.K.; Yurtcan, A.B. Investigation of the Thermal Behavior of Polypyrrole/Carbon Nanotube Composites and Utilization as Capacitive Material or Support for Catalysts. *Chem. Eng. Commun*. **2017,** 204, 916-925.

[22]Cai, H.; Xu,Y.; He, P.G.; Fang, Y.Z. Indicator Free DNA Hybridization Detection by Impedance Measurement Based on the DNA - Doped Conducting Polymer Film Formed on the Carbon Nanotube Modified Electrode. *Electroanalysis* **2003**, *15*, 1864-1870.

[23]Gupta, S.; Murthy, C.N.; Ratna, P.C. Recent advances in carbon nanotube based electrochemical biosensors. *Int. J. Biol. Macromol*.**2018,** 108, 687–703.

[24]Cheraghi, S.; Taher, M.A.; Karimi-Maleh, H.; Faghih-Mirzaeide, E. A nanostructure label-free DNA biosensor for ciprofloxacin analysis as a chemotherapeutic agent: an experimental and theoretical investigation. *New*. *J. Chem.* **2017**, 41, 4985-4989.

[25]Arulraj, A.D.; Sundaram, E.; Vasantha, V.S.; Neppolian, B. Polypyrrole with a functionalized multi-walled carbon nanotube hybrid nanocomposite: a new and efficient nitrite sensor. *New J. Chem*., **2018**, 42, 3748-3757.

[26]Eom, G.; Oh, C.; Moon, J.; Kim, H.; Kim, M.K.; Kim, K.; Seo, Ji-W.; Kang,T.; Lee, H.J. Highly sensitive and selective detection of dopamine using overoxidized polypyrrole/sodium dodecyl sulfate-modified carbon nanotube electrodes. *J. Electroanal. Chem.* **2019**, 848, 113295

[27]Oularbi, L.; Turmine, M.; Rhazia, M.E. Preparation of novel nanocomposite consisting of bismuth particles, polypyrrole and multi-walled carbon nanotubes for simultaneous voltammetric determination of cadmium(II) and lead(II). *Synth. Met.* **2019**, 253,1-8.

[28] Lo, M.; Diaw, A.K.D.; Gningue-Sall, D.; Aaron, J-J.; Oturan, M.A.; Chehimi, M.M. The role of diazonium interface chemistry in the design of high performance polypyrrole-coated flexible ITO sensing electrodes. *Electrochem. Commun*. **2017,** 77, 14-18.

[29] Lo, M.; Pires, R.; Diaw, K.; Gningue-Sall, D.; Oturan, M. A.; Aaron, J. J.; Chehimi, M. M. (2018). Diazonium salts: versatile molecular glues for sticking conductive polymers to flexible electrodes. *Surfaces.***2018**, *1*, 43–58.

[30] C. Perruchot, M. M. Chehimi, M. Delamar, E. Cabet-Deliry, B. Miksa, S. Slomkowski,

Preprints (www.preprints.org) | NOT PEER-REVIEWED | Posted: 17 November 2019 doi:10.20944/preprints201911.0211.v1

M. A. Khan and S. P. Armes, *Colloid Polym. Sci.*, 2000, 278, 1139.

[31] Mohamed, A. A.; Salmi, S. ; Dahoumane, S. A. ; Mekki, A.; Carbonnier, B. ; Chehimi, M. M. Functionalization of nanomaterials with aryldiazonium salts. *Adv. Colloid Interface Sci*. **2015**, *225*, 16-36.

[32] Lo, M.; Diaw, A.K.D.; Gningue-Sall, D.; Aaron, J.-J.; Oturan, M.A.; Chehimi, M.M. Tracking metal ions with polypyrrole thin films adhesively bonded to diazonium-modified flexible ITO electrodes. *Environ. Sci. Pollut. Res*. **2018**, 25, 20012–20022.

[33]Hong, J., Pintauro, P. N. Selective removal of heavy metals from contaminated kaolin by chelators. *Water, Air, Soil Pollution*, **1996**, 87, 73-91.

[34] Bhakta, A.K.; Detriche, S.; Martis, P.; Mascarenhas, R.J.; Delhalle, J.; Mekhalif, Z. Decoration of tricarboxylic and monocarboxylic aryl diazonium functionalized multi-wall carbon nanotubes with iron nanoparticles. *J. Mater. Sci.***2017,** 52, 9648–9660.

[35] Fu, X.-C.; Wu, J.; Nie, L.; Xie, C.-G.,Liu, J.-H. ; Huang, X.-J. Electropolymerized surface ion imprinting films on a gold nanoparticles/single-wall carbon nanotube nanohybrids modified glassy carbon electrode for electrochemical detection of trace mercury(II) in water. *Anal. Chim. Acta.***2012**, 720, 29-37.

[36]Tasis, D.; Tagmatarchis, N. ; Bianco, A. ; Prato, M. Chemistry of carbon nanotubes. *Chem. Rev*. **2006,** 106, 1105-1136.

[37]Yu, S.S.C.; Tan, E.S.Q.; Jane, R.T.; Downard, A.J. An electrochemical and XPS study of reduction of nitrophenyl films covalently grafted to planar carbon surfaces. *Langmuir*. **2007**, 23, 11074-11082.

[38]Pilan, L.; Raicopol, M.; Pruna, A.; Branzoi, V. Polyaniline/carbon nanotube composite filmselectrosynthesis through diazonium salts electroreduction and electrochemical polymerization. *Surf. Interface Anal.***2012**, 44, 1198–1202.

[39]Liu, Y-C.; McCreery, R.L.; Reactions of Organic Monolayers on Carbon Surfaces Observed with Unenhanced Raman Spectroscopy, *J. Am. Chem. Soc.***1995**,117, 11254-11259

[40]Song, H.; Cai, K.; Wang, J.; Shen, S.; Influence of polymerization method on the thermoelectric properties of multi-walled carbon nanotubes/polypyrrole composites. *Synt.Met.***2016,** 211, 58-65.

[41] Afzal, A.; Abuilaiwi, F.A.; Habib, A.; Awais, M.; Waje, S.B.; Atieh, M.A. Polypyrrole/carbon nanotube supercapacitors: Technological advances and challenges, *J. Power Sources.* **2017**, 352, 174-186.

[42]Bensghaïer, A.; Truong, S.L.; Seydou, M.; Lamouri, A.; Leroy, E.; Matej, M.; Forro, K.; Beji, M.; Pinson, J.; Omastova, M.; Chehimi, M.M. Efficient Covalent Modification of Multiwalled Carbon Nanotubes with Diazotized Dyes in Water at Room Temperature, *Langmuir*. **2017**, 33, 6677–6690.

[43] Hicks, M.; Wong, Z.Y.; Scurr, D.J.; Silman, N.; Jackson, S.K.; Mendes, P.M.; Aylott, J.W.; Yi, Z.; Rawson F.J. Tailoring the Electrochemical Properties of Carbon Nanotube Modified Indium Tin Oxide via in Situ Grafting of Aryl Diazonium. *Langmuir*, **2017**, 33, 4924−4933.

[44]Chamjangali, M.A.; Kouhestani, H.; Masdarolomoor, F.; DaneshinejadH.;A voltammetric sensor based on the glassy carbon electrode modified with multi-walled carbon nanotube/poly(pyrocatecholviolet)/bismuth film for determination of cadmium and lead as

Preprints (www.preprints.org) | NOT PEER-REVIEWED | Posted: 17 November 2019 doi:10.20944/preprints201911.0211.v1

environmental pollutants. *Sens. Actuators* B. **2015**, 216, 384–393.

[45]Lee, C.; Yang, W.; Parr, R. G. Development of the Colle-Salvetti correlation-energy formula into a functional of the electron density. *Phys. Rev. B*,**1988**, *37*, 785-789.

[46] Frisch, M. J., Trucks, G. W, Schlegel, H. B., Scuseria, G. E., Robb , M. A., Cheeseman, J. R., Scalmani, G., Barone, V., Mennucci, B., Petersson, G. A., Nakatsuji, H., Caricato, M., Li, X., Hratchian, H. P., Izmaylov, A. F., Bloino, J., Zheng, G., Sonnenberg, J. L., Hada, M., Ehara, M ., Toyota, K., Fukuda, R., Hasegawa, J., Ishida, M., Nakajima, T., Honda, Y., Kitao, O., Nakai, H., Vreven, T., Montgomery, J. A. Jr, Peralta, J. E., Ogliaro, F., Bearpark, M., Heyd, J. J., Brothers, E., Kudin, K. N., Staroverov, V. N., Kobayashi, R., Normand, J., Raghavachari, K., Rendell, A., Burant, J. C., Iyengar, S. S., Tomasi, J., Cossi, M., Rega, N., Millam, J. M., Klene, M., Knox, J. E., Cross, J. B., Bakken, V., Adamo, C., Jaramillo, J., Gomperts, R., Stratmann, R. E., Yazyev, O., Austin, A. J., Cammi, R., Pomelli, C., Ochterski, J. W., Martin, R. L., Morokuma, K., Zakrzewski, V. G., Voth, G. A., Salvador, P., Dannenberg, J. J., Dapprich, S., Daniels, A. D., Farkas, Ö., Foresman, J. B., Ortiz, J. V., Cioslowski, J., Fox, D.J. 2009. Gaussian, Inc., Wallingford CT.

[47]Dasent, pps. 44-47; Moore,C.E. "National Standard Reference Data Series," National Bureau of Standards, No. 34, Washington, DC, 1970; Martin, W.C.;Hagan, L.;Reader, J.;Sugar, J. *J. Phys. Chem. Ref. Data*, 1974, 3, 771-779.

[48]Barone, V.;Cossi, M.;Tomasi, J. A New definition of cavities for the computation of solvation free energies by the polarizable continuum model. *J. Chem. Phys.*, 1997,107, 3210-3221.